Adam MUC[1]

Uniwersytet Morski w Gdyni, Katedra Automatyki Okrętowej (1)
ORCID: 1. 0000-0002-9495-087X

doi:10.15199/48.2024.10.53

Cooperation of various levels and three-phase voltage inverters using the theory of orthogonal space vectors

***Abstract**. This paper presents the concept of cooperation of different multilevel and three-phase inverters using orthogonal space vector theory. The resulting converter is built from two inverters, one of which is a three-level (main) inverter and the other a two-level (auxiliary) inverter. The case presented in the article focuses on increasing the levels of the three-phase stepped output voltage and reducing the content of higher harmonics. The simulation results obtained prove the assumptions made about the shape of the output voltages and the value of the THD coefficient.*

***Streszczenie.** W artykule przedstawiono koncepcję współpracy różnych, wielopoziomowych i trójfazowych falowników z wykorzystaniem teorii przestrzennych wektorów ortogonalnych. Powstały w ten sposób przekształtnik zbudowany jest z dwóch falowników, z których jeden jest falownikiem trójpoziomowym (głównym) a drugi dwupoziomowym (pomocniczym). Przedstawiony w artykule przypadek koncentruje się na zwiększeniu poziomów trójfazowego, schodkowego napięcia wyjściowego i obniżeniu zawartości wyższych harmonicznych. Uzyskane wyniki badań symulacyjnych dowodzą przyjętych założeń dotyczących kształtu napięć wyjściowych i wartości współczynnika THD. **(Współpraca różnych - co do liczby poziomów i trójfazowych falowników napięcia z wykorzystaniem teorii przestrzennych wektorów ortogonalnych**).*

Keywords: space vector; vector orthogonality; three-phase OVT inverter; fundamental harmonic.
Słowa kluczowe: wektor stanów, wektor ortogonalny, trójfazowy falownik OVT, harmoniczna podstawowa.

Introduction

The development of renewable energy sources and electromobility are currently the main reasons driving evolution in power electronics, which are contributing to the emergence of circuit solutions geared toward the cooperation of different converters and the conditioning of electricity. These aspects are fundamental when considering the possibilities of connecting the RES (Renewable Energy Source) network to the existing power system [1].

The conversion DC/AC directly into alternating current is one of the most essential targets of contemporary power electronics. Such a necessity is required in AC drives and in the area of renewable energy applications e.g. smart grids. In both domains, the critical parameters that should be regulated are voltage amplitude and frequency although the regulation range of these parameters is quite different. A typical control system in AC drives includes an inverter acting as a DC/AC converter. The most practical control method PWM (pulse-width modulation) causes the output voltage to take the form of rectangular pulses. Therefore, to receive a sine wave voltage, it is usually obligatory to use a low band filter which is capable of selecting a fundamental harmonic voltage component [3].

In the cases mentioned, one of the most important components of the system is the inverter. The paper [4] provides a comprehensive overview of the different types of inverters currently used in various applications and variants of power systems. Generally, a traditional voltage-fed inverter is used, where two voltage levels can be generated [5]. For other applications, especially those requiring high power conversion (e.g., on-shore power supply systems), multi-level inverters (MLIs) are used. An MLI is a converter system in which different types of power electronic devices are interconnected in such a way and are fed from DC systems to provide a waveform with more levels on the output side [6,7]. MLI circuits are desirable for a variety of applications due to intrinsic benefits, for example, low switching voltages, low DV/DT ratio on switches, reliability, lower cost, reduced complexity, improved THD, and exceptional performance when used in applications [8,9].

Since the use of multilevel inverters has begun, numerous layout changes have been made to the inverters. Their control strategies have also changed. This has resulted in increased circuit complexity, weight, and cost; stress on switches; electromagnetic compatibility (EMC)/ electromagnetic interference (EMI) problems; and circuit losses. These effects lead to performance degradation and affect the nature of power in network/distribution systems. For this reason, traditional bilevel inverters are still very popular in low-power systems [4].

Various modulation schemes are available and are used to build control strategies for inverter operations [10,11]. A significant proportion of the modulators used for inverters are based on pulse width modulation (PWM) modifications. Modulations using PWM mainly increase the switching losses of the electronic switches used in inverters [12–14].

As mentioned earlier, the use of multi-level inverters and appropriate control strategies allows for multiple levels of output voltages. Multi-level voltage is usually associated with lower THD and better power quality [15]. As it has been shown, obtaining such a voltage requires the use of complex inverter structures and complicated control strategies based on a large number of electronic switches [16].

The development of a converter with multiple inverters in the form of a three-phase system requires the analysis of systems that allow for the integration of multiple inverters in one system. For this purpose, systems based on transformers, multi-winding transformers, and systems using magnetically coupled reactors were compared [17–18].

However, there are some stimulating possibilities concerning DC/AC converters constructed of two inverters, which are considered, for this paper, as orthogonal-vectors-controlled inverters (OVTs). The main advantages and disadvantages of the control concept based on orthogonal vectors have been presented and discussed in [19, 20]. The original control method of the auxiliary inverter didn't remain very efficient. The use of a transformer transferring relatively long pulses was the main disadvantage of the presented solution. A novel idea of the auxiliary inverter control method has been developed and described in [21]. The paper [21] presents a novel, modified proposal regarding the OVT inverter control method. The recommended control method brought a significant reduction in the transformer size used as a summing node of the OVT inverter.

The article presents a unique possibility of cooperation between a three-level inverter and a two-level inverter. This solution, unlike the previous ones which used only two-level inverters, is characterized by the ability to transfer higher power, lower THD, and new control options.

The OVT inverter idea

The basic block diagram of the OVT inverter is shown in Figure 1. The main idea and performance of the inverter have been developed and presented in publications [13, 14, 15, 16] as well as the modified proposal in work [17]. Made of two inverters: main (MI) - three-level and auxiliary (AI) - two-level. The main inverter created in this way generates 32 spatial voltage vectors of similar length. The component inverters are connected to a combination of single-phase transformers and are powered by a single DC voltage source. An important element of this structure is the summing node made in the form of the three mentioned single-phase transformers. A star connection is used on the main inverter and load side, and a delta connection is used on the auxiliary inverter side. This means that the phase voltage of the main inverter is shaped by the phase-to-phase voltage of the auxiliary inverter.

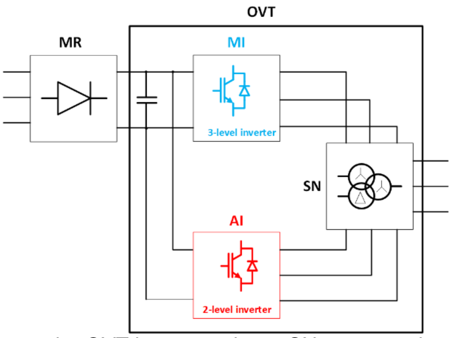

Fig.1. Scheme the OVT inverter, where: SN – sum node, MR - main rectifier

Next figure 2 determines the rule of vector creation. The vectors are denoted as:

- V_{MIk} — the main inverter voltage vector k;
- V_{AIk} —the auxiliary inverter voltage vector k;
- V_{OVTk} — the OVT inverter voltage vector k

and k = 1, 2, 3 …, 32.

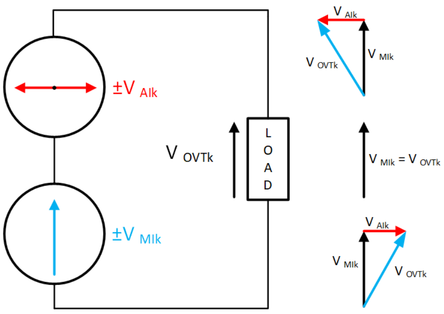

Fig.2. The formation concept of vectors V_{OVTk}

The vectors VMI_k and VAI_k are mutually orthogonal and presented in Figure 3. Figure 3 shows selected vectors of a three-level inverter - an inverter with an NPC (Neutral Point Clamped) structure. Vectors marked as VMI13, ..., and VMI18 are the longest vectors of the inverter, and vectors marked as VMI12, ..., and VMI7 belong to the group of medium vectors. The adopted variant did not consider short vectors. Figure 3 also shows the vectors of the AI (two-level) inverter, which were placed in the α, β system and were shifted by an angle π/2 relative to the vectors of the MI (three-level) inverter. An important element of Figure 3 is an illustration that shows the arrangement of orthogonal vectors for an example sequence of MI and AI vectors creating a domain of orthogonal vectors. The example concerns the vector VOVT_MI13 and VOVT_MI13<->AI5 AND VOVT_MI13<->AI1.In every of six k-sectors of the stationary coordinate system plane (α, β) the OVT inverter generates a sequence of three voltage vectors: V_(OVT-), V_OVT, V_(OVT+), assigned to the k-th sector of the plane (α, β). The order of generation is described in equation (1):

$$(1)\quad \begin{gathered} \underset{\rightarrow Ok-}{\boldsymbol{V}} = \underset{\rightarrow Ak\oplus 3}{\boldsymbol{V}} + \underset{\rightarrow Mk}{\boldsymbol{V}} \\ \underset{\rightarrow Ok}{\boldsymbol{V}} = \underset{\rightarrow Mk}{\boldsymbol{V}} \\ \underset{\rightarrow Ok+}{\boldsymbol{V}} = \underset{\rightarrow Ak}{\boldsymbol{V}} + \underset{\rightarrow Mk}{\boldsymbol{V}} \end{gathered}$$

The symbol k⊕3 denotes the modulo 6 sum of the index k and the number 3. Expression (1) illustrates a control method based on the principle of orthogonal vector summation. In the stationary coordinate system (α, β) the active vectors of the component inverters are described by expressions (2).

$$(2)\quad \begin{cases} \underset{\rightarrow Mk}{\boldsymbol{V}} = \left|\underset{\rightarrow Mk}{\boldsymbol{V}}\right| e^{j\,\left[(k-1)\frac{\pi}{3} \pm 2\pi n\right]} \\ \underset{\rightarrow Ak}{\boldsymbol{V}} = \pm\, jm\,\underset{\rightarrow Mk}{\boldsymbol{V}} = \pm\, m\,\underset{\rightarrow Mk}{\boldsymbol{V}}\, e^{j\,\frac{\pi}{2}} \end{cases}$$

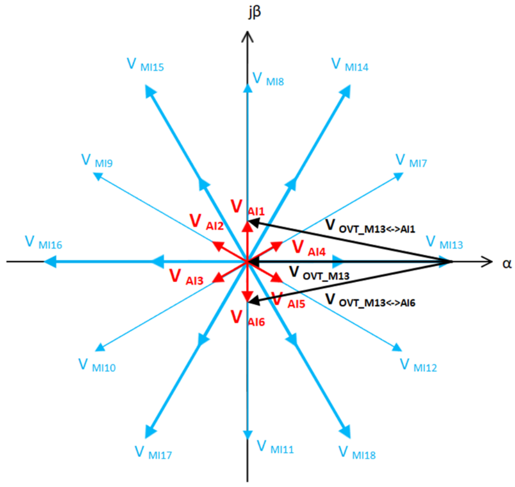

Fig.3. The active vectors of the main and auxiliary inverters

According to equations (1, 2), the output space vectors of the OVT orthogonal converter are given by relations (3).

$$(3)\quad \begin{cases} \underset{\rightarrow Ok-}{\boldsymbol{V}} = (1 - jm)\,\underset{\rightarrow Mk}{\boldsymbol{V}} = \sqrt{1+m^2}\,\underset{\rightarrow Mk}{\boldsymbol{V}}\, e^{-j\cdot arctan\, m} \\ \underset{\rightarrow Ok}{\boldsymbol{V}} = \underset{\rightarrow Mk}{\boldsymbol{V}} = \left|\underset{\rightarrow Mk}{\boldsymbol{V}}\right| e^{j\,\left[(k-1)\frac{\pi}{3} \pm 2k\,\pi\right]} \\ \underset{\rightarrow Ok+}{\boldsymbol{V}} = (1 + jm)\,\underset{\rightarrow Mk}{\boldsymbol{V}} = \sqrt{1+m^2}\,\underset{\rightarrow Mk}{\boldsymbol{V}}\, e^{\,j\cdot arctan\, m} \end{cases}$$

If it is assumed that the output vectors are switched on at equal time intervals, the ratio of the lengths of the vectors is equal to (4).

$$(4)\qquad m = \frac{\left|\underset{\rightarrow Ak}{\boldsymbol{V}}\right|}{\left|\underset{\rightarrow Mk}{\boldsymbol{V}}\right|} = tg\,\left(\frac{\pi}{18}\right) = 0.176$$

	V11	V11	V11	V18	V18	V18	V12	V12	V12	V13	V13	V13	V7	V7	V7	V14	V14	V14	V8	V8	V8	V15	V15	V15	V9	V9	V9	V16	V16	V16	V10	V10	V10	V17	V17	V17
TMIa1	0	0	0	1	1	1	1	1	1	1	1	1	1	1	1	1	1	1	0	0	0	0	0	0	0	0	0	0	0	0	0	0	0	0	0	0
TMIa2	1	1	1	1	1	1	1	1	1	1	1	1	1	1	1	1	1	1	1	1	1	0	0	0	0	0	0	0	0	0	0	0	0	0	0	0
TMIa3	1	1	1	0	0	0	0	0	0	0	0	0	0	0	0	0	0	0	1	1	1	1	1	1	1	1	1	1	1	1	1	1	1	1	1	1
TMIa4	0	0	0	0	0	0	0	0	0	0	0	0	0	0	0	0	0	0	0	0	0	1	1	1	1	1	1	1	1	1	1	1	1	1	1	1

	V7	V7	V7	V3	V7	V4	V0	V0	V0	V1	V0	V6	V7	V7	V7	V5	V7	V2	V0	V0	V0	V6	V0	V1	V7	V7	V7	V6	V7	V1	V0	V0	V0	V2	V0	V5
TAIa1	1	1	1	0	1	1	0	0	0	0	0	1	1	1	1	1	1	0	0	0	0	1	0	0	1	1	1	1	1	0	0	0	0	0	0	1
TAIa2	0	0	0	1	0	0	1	1	1	1	1	0	0	0	0	0	0	1	1	1	1	0	1	1	0	0	0	0	0	1	1	1	1	1	1	0

Fig.4. The map of the control vectors of the first-phase transistors in MI and AI inverters.

Figure 4 shows a map of the space vectors controlling the transistors in phase "a" of the main and auxiliary inverters. Then, theoretical voltage waveforms were shown, i.e. phase voltage "a" for the MI inverter, phase-to-phase voltage "ba" for the AI inverter, and phase voltage "a" for the OVT inverter. Figure 5 also shows that the space vectors of the auxiliary inverter are generated three times more often in one plan sector (α, β), so the frequency of the AI vector is three times higher than the frequency of the MI vector.

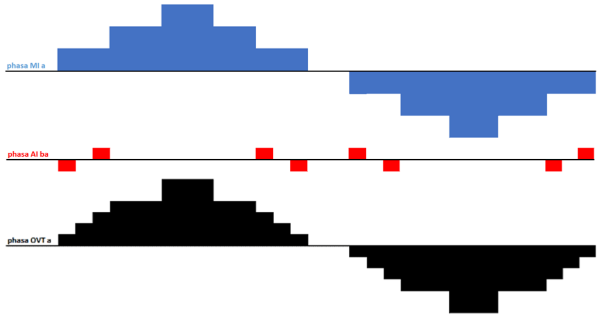

Fig.5. The theoretical voltage waveforms of MI, AI and OVT inverters

Simulation model and operation principle

Figure 6 shows a diagram that illustrates the connection of a three-level inverter with a two-level inverter. The presented model was used in simulation studies. The diagram shows the modulator blocks responsible for forming control signals consistent with the spatial vectors shown in Figures 2 and 3, the topology of the three-level and two-level inverter, the summing node in the form of three single-phase transformers with a 1:6 ratio, and the resistive-inductive load.

Results of simulation tests

Simulation tests were performed in the PLECS program and the RT Box device. The PLECS program is a dedicated program for modeling power electronic converters, while the RT Box is a device that allows conducting simulation tests in the processor loop (PIL).

Table 1 presents a collection of selected voltage parameters recorded in the presented converter. The table shows the RMS value and the value of the THD coefficient.

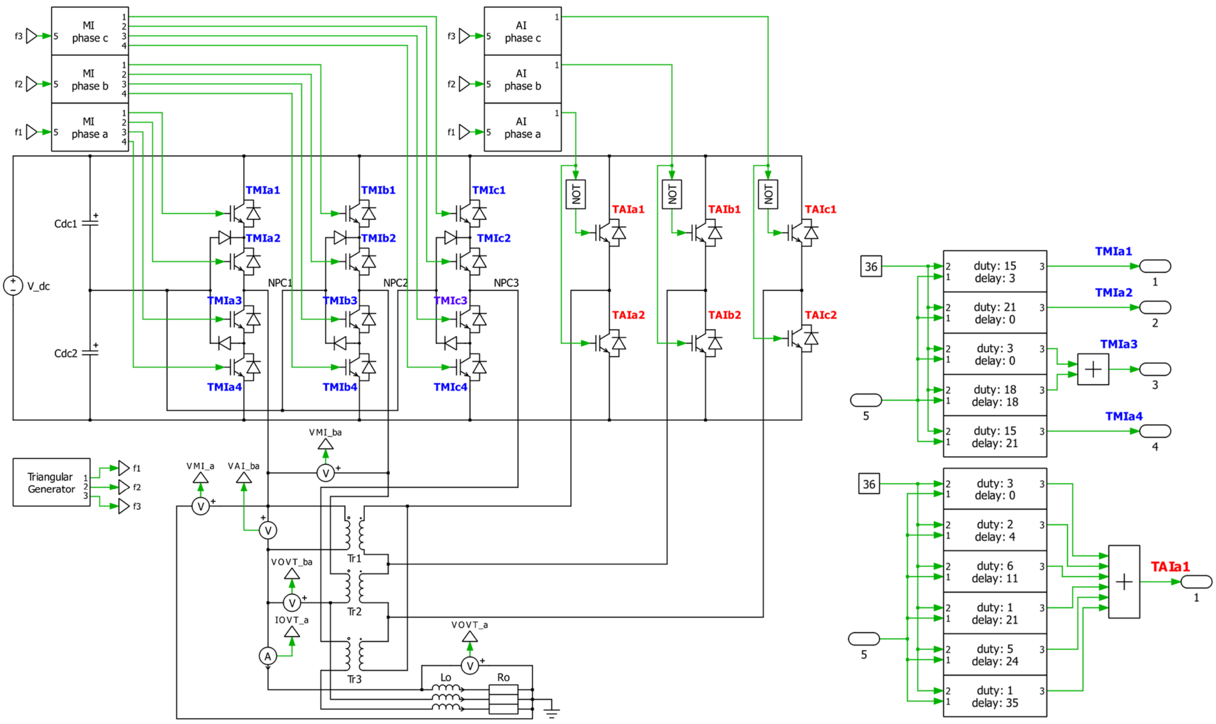

Fig.6. The complete converter diagram and blocks that form signals MI phase a and AI phase a

Table 1. Selected parameters of recorded voltages at 40 Hz

Waveform	RMS (V)	THD (%)
VAI_ba	29.64	99.3
VMI_a	167.01	18.8
VOVT_a	169.62	12.3
VMI_ba	289.27	18.5
VOVT_ba	293.79	13.1

The use of the concept of orthogonal vectors to control a three-level and two-level inverter allowed for an increase in the RMS voltage value and a reduction in THD. Please note that the article presents the simplest configuration of vectors. By selecting other variants of vectors, you will be able to achieve better results.

Figure 7 shows selected voltage waveforms and Figure 8 shows their amplitude spectra.

The voltage spectra: VOVT_a and VOVT_ba, shown in Figure 8, are characterized by the presence mainly of the fundamental harmonic. This effect was achieved without the use of PWM modulation.

Conclusions

The presented OVT inverter is designed to support an efficient DC/AC conversion process. The total power of the OVT inverter can be very high, as can the MI power, but the power of the AI inverter remains relatively low. As a result, the power losses of the entire OVT inverter, as well as the MI and AI component inverters, are very low. In the adopted control strategy, the main MI inverter is switched only four times per harmonic voltage period. This allows the control circuit of the complete OVT inverter to operate most simply. Other control strategies can also be considered that may bring even better results. The OVT inverter is capable of controlling the frequency and amplitude of the output voltage simultaneously but requires another version of the modulator. The proposed converter concept also seems to be an interesting proposition in the hardware context, because the two-level inverter modules or even three-level ones are now cheaper and easily available. Moreover, adding PWM modulation in the control system will result in smaller transformers used as a summing node due to the voltage switching frequency for the AI inverter. The THD coefficients of voltage and current meet the limits of EN: 50160.

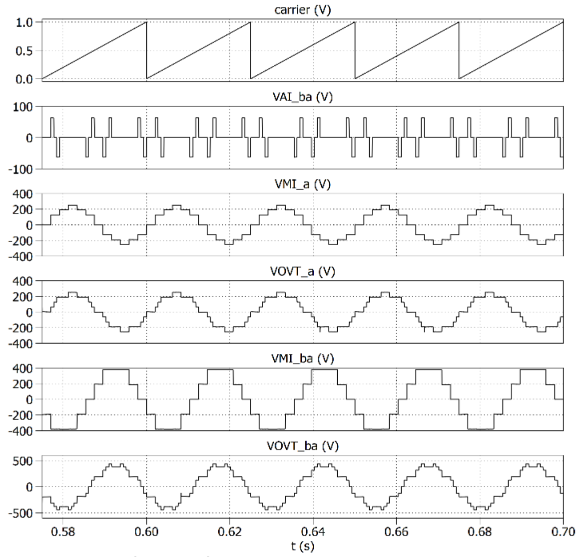

Fig.7. The waveforms of selected voltages recorded in the inverter system recorded for a frequency of 40 Hz

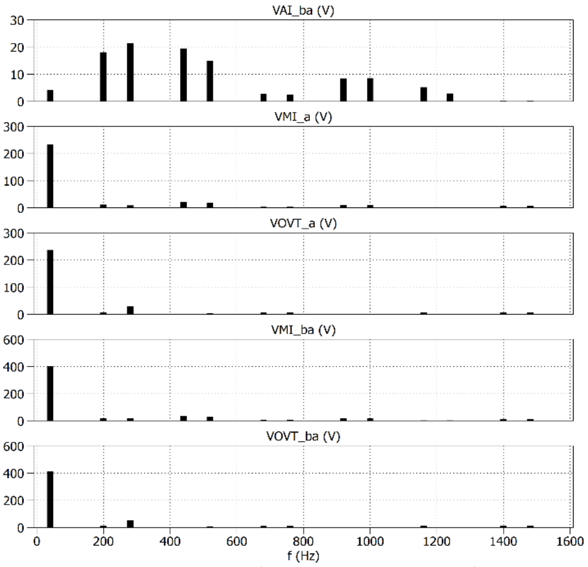

Fig.8. Amplitude spectra of selected voltages from Figure 7 showing 40 harmonics

***Authors**: dr inż. Adam Muc, E-mail: a.muc@we.umg.edu.pl; Uniwersytet Morski w Gdyni, Katedra Automatyki Okrętowej, Wydział Elektryczny, ul. Morska 81-87, 81-225 Gdynia.*

REFERENCES

[1] B.K. Bose, Power Electronics, Smart Grid, and Renewable Energy Systems. Proc. IEEE 2017, 105, 2011–2018. https://doi.org/10.1109/JPROC.2017.2745621.

[2] A. Łebkowski, Steam and Oxyhydrogen Addition Influence on Energy Usage by Range Extender—Battery Electric Vehicles. Energies 2018, 11, 2403. https://doi.org/10.3390/en11092403.

[3] X. Hu, J. Wang, L. Li, Y. Li, A Three-Winding Coupled-Inductor DC–DC Converter Topology With High Voltage Gain and Reduced Switch Stress. IEEE Trans. Power Electron. 2018, 33, 1453–1462 https://doi.org/10.1109/TPEL.2017.2689806.

[4] K.N.D.V.S Eswar, M.A.N.Doss, P.Vishnuram, A.Selim, M.Bajaj, H.Kotb, S. Kamel, Comprehensive Study on Reduced DC Source Count: Multilevel Inverters and Its Design Topologies. Energies 2023, 16, 18. https://doi.org/10.3390/en16010018.

[5] G.G. Kumar, M.V.S. Krishna, S. Kumaravel, E. Babaei, Multi-Stage DC-DC Converter Using Active LC2D Network With Minimum Component. IEEE Trans. Circuits Syst. II: Express Briefs 2021, 68, 943–947. https://doi.org/10.1109/TCSII.2020.3021609.

[6] K.N. Raju, M.V.G. Rao, M. Raamoorthy, Hybrid moulation technique for neutral point claped inverter to eliminate neutral 500 point shift with minimum swithing loss. In Proceedings of the TENCON 2015—2015 IEEE Region 10 Conference, Macao, China, 1–4 November 2015; pp. 1–5. https://doi.org/10.1109/TENCON.2015.7373101.

[7] Z.Xu, X. Zheng, T. Lin, J.Yao, A.Ioinvici, Switched-capacitr multilevel inverter with equal distrbution of the capacitors discharging phases. J. Electr. Eng. 2020, 6, 42–52. https://doi.org/10.23919/CJEE.2020.000029. (In Chinese)

[8] A.K.Yadav, K. Gopakumar, L. Umanand, S.Bhattacharya, W. A Jarzyna, Hybrid 7-Level Inverter Using Low-Voltage Devices and Operation With Single DC-Link. IEEE Trans. Power Electron. 2019, 34, 9844–9853. https://doi.org/10.1109/TPEL.2018.2890371.

[9] L.Dorn-Gomba, J. Guo, A. Emadi, Multi-Source Inverter for Power-Split Hybrid Electric Powertrains. IEEE Trans. Veh. Technol. 2019, 68, 6481–6494. https://doi.org/10.1109/TVT.2019.2915173.

[10] M.D. Siddique, Low Switching Frequency Based on Asymmetrical Multilevel Inverter Topology With Reduced Switch Count. IEEE Access 2019, 7, pp. 86374–86383.

[11] G.H.P. GOoi, A.I. Maswood, Z. Lim, Five-Level Multiple-Pole PWM AC–AC Converters With Reduced Components Count. IEEE Trans. Ind. Electron. 2015, 62, 4739–4748. https://doi.org/10.1109/TIE.2015.2405504.

[12] R. Sarker, A. Datta, S. A Debnath, Modified PWM Technique to Reduce Harmonic Content of Multilevel NPC Topology 769 for Medium Voltage Electric Vehicle (EV) Applications. In Proceedings of the Michael Faraday IET International Summit 2020 (MFIIS 2020), Online, 3–4 October 2020, Volume 770, pp. 19–22.

[13] T.R.Por, A.A. Rathd, S.K. Patil, Performance Analysis of Cascaded H-Bridge Multilevel Inverter with Variable Frequency ISPWM Technique. In Proceedings of the 2019 Innovations in Power and Advanced Computing Technologies (i-PACT), Vellore, India, 22–23 March 2019.

[14] A. Muc, J. Iwaszkiewicz, Scalar Voltage-Frequency Control of the OVT Inverter. Prz. Elektrotechniczny 2023, 99, 217–220. https://doi.org/10.15199/48.2023.09.42.

[15] B. Jyothi, A. Pandian, P. Bhavana, Fabrication and experimental analysis of multiple-winding transformers for multiphase supply. Meas. Control. 2020, 53, 662–678. https://doi.org/10.1177/0020294019897086.

[16] T.F. Dorazio, High phase order transmission. In Proceedings of the 1990 IEEE technical conference on Southerntier, Binghamton, NY, USA, 25 April 1990; IEEE: New York, NY, USA.

[17] A. Singh, J.R. Marti, Srivastava, K.D. Circuit reduction techniques in multiphase modelling of power transformers. IEEE Trans. Power Deliv. 2010, 25, 1573–1579.

[18] A.Munteanu, A.Simion, D.A. Hagianu, L. Livadaru, D. Bidei, Special three-phase to multiple different polyphase systems electric transformer. In Proceedings of the 2014 International Conference and Exposition on Electrical and Power Engineering (EPE), Iasi, Romania, 16–18 October 2014; IEEE: New York, NY, USA.

[19] M. Hartman, M. Hashad, J. Iwaszkiewicz, Developing Inverter Output Voltage Waveforms with the Help of Orthogonal Space Vectors, IEE Conference Power Electronics and Variable Speed Drives PEVD'2000, London, United Kingdom, 18–19 IX 2000.

[20] M. Hashad, J. Iwaszkiewicz, A Novel Orthogonal-Vectors-Based Topology of Multilevel Inverters. IEEE Trans. Ind. Electron. 2002, 49, pp. 868–874.

[21] A. Muc, J. Iwaszkiewicz, Active Filtering of Inverter Output Waveforms Based on Orthogonal Space Vector Theory, Energies 2022, 15(21), 7861, https://doi.org/10.3390/en15217861.